Embedment Depth Influence on an Uplifting Anchor

Jinyuan Liu[1], M. ASCE and Mingliang Liu[2]

[1]Assistant Professor, Ryerson University, Toronto, Canada; jinyuan.liu@ryerson.ca
[2]Graduate Research Assistant, Hohai University, Nanjing, China; mingliang.liu79@gmail.com

ABSTRACT: This paper presents an experimental investigation on the influence of embedment depth on the anchor failure mode. It is widely understood that a deep anchor will behave differently compared to a shallow anchor. A test set-up is developed in this research to capture soil deformation during anchor uplifting, which consists of a camera, a loading frame, a Plexiglas mould, and a computer. A series of model tests are performed to investigate the influence of the anchor embedment depth on soil deformation. A set of images are captured while a semi-circular anchor is being uplifted against the Plexiglas window. A soil displacement field is calculated from two images using the Digital Image Correlation (DIC) method. The failure surface is studied by locating the maximum shear strains deduced from the soil displacement field. Based on this study, it is found that the anchor behaviour is substantially influenced by the anchor embedment depth. A similar punching failure mode is observed in loose sand regardless of the anchor depth. However, in dense sand a restrained failure mode is observed in a deep anchor opposite to the mode with failure plane extending to ground surface in a shallow anchor. This study improves the understanding of soil-anchor interaction and helps to design an efficient anchor system.

INTRODUCTION

Anchors, as an efficient and reliable anchorage system, have been widely used to resist uplift loads produced by structures such as transmission towers, offshore platforms, submerged pipelines and tunnels. With the extensive use of anchors in foundation systems, the understanding of their behaviour has attracted the attentions of researchers for more than half a century (Balla 1961; Sutherland 1965; Meyerhof and Adams 1968; Vesic 1971; Saeedy 1987; Murray and Geddes 1987). Many testing methods have been used to study the behaviour of anchor, including large-scale field testing, laboratory model testing, and theoretical analyses. Many of these tests and analyses have been performed to understand the failure mode in an earth anchor (Ilamparuthi et al. 2002) and displacement fields (Carr and Hanna 1971).

It is widely understood that a deep anchor will behave differently compared to a shallow anchor. However, limited information is available in visualizing soil deformation around an uplifting anchor and change of soil deformation with anchor embedment depth. This study investigates the change of anchor behaviour with the embedment depth in sand using the Digital Image Correlation (DIC) method.

EXPERIMENTAL SET-UP AND TEST PROCEDURE

Equipment Set-up

An experimental test set-up is developed in this research, which consists of a mono complementary metal–oxide–semiconductor (CMOS) camera, a test table, a loading frame, a Plexiglas mould, and a PC, as schematically shown in Fig. 1. The camera is PixeLink PL-B741E model camera with a resolution of 1280 x 1024 pixels from PixeLink. A built-in lens in the camera is used to adjust the focus. The camera is set 15 cm away from the model with its optical axis perpendicular to the model. It is controlled by the PC through an in-house developed driver using Matlab® Simulink commands. The frame rate for image capturing is set as 1 frame per second during uplifting.

The loading frame consists of a load cell with a loading capacity of 500 N and a linear displacement transducer (LVDT) with a linear strike of ± 25 mm. A data acquisition system has been developed to acquire the loads and displacements of the anchor during uplifting, which consists of NI-6011E PC card and SCB-68 shielded connector from National Instruments and an in-house developed driver in Labview.

The Plexiglas mould has dimensions of 800 mm (length) x 500 mm (width) x 500 mm (depth). A semicircular anchor with a diameter of 50 mm and a thickness of 6 mm is used in this study. A 1 m long and 6 mm diameter threaded steel rod is used to connect the anchor. The anchor is tightened in between by two screws attached to the top and bottom of the model anchor. The rod is then connected to the loading frame through an adaptor. The load cell and the LVDT are attached to the rod to measure the load and deformation of the anchor during uplifting, as shown in Fig. 1.

Load was applied vertically through a screw mechanism. The anchor is lifted along a guide slot upward by manually rotating the handle while the images and the load and deformation are acquired simultaneously.

Soil Properties

In order to study the influence of soil density, two conditions are investigated in this research; one is loose and the other is dense. The maximum dry unit weight is tested at 16.95 KN/m^3 according to ASTM D-698. The minimum dry unit weight is tested at 13.8 KN/m^3 by pouring from a funnel. The soil conditions with dry unit weights of 14.6 KN/m^3 and 16.0 KN/m^3 are used in the tests, which represent relative density of 27 % and 71 %. Typical soil properties are shown in Table. 1. The sand is classified as SP uniformly graded according to Unified Soil Classification System.

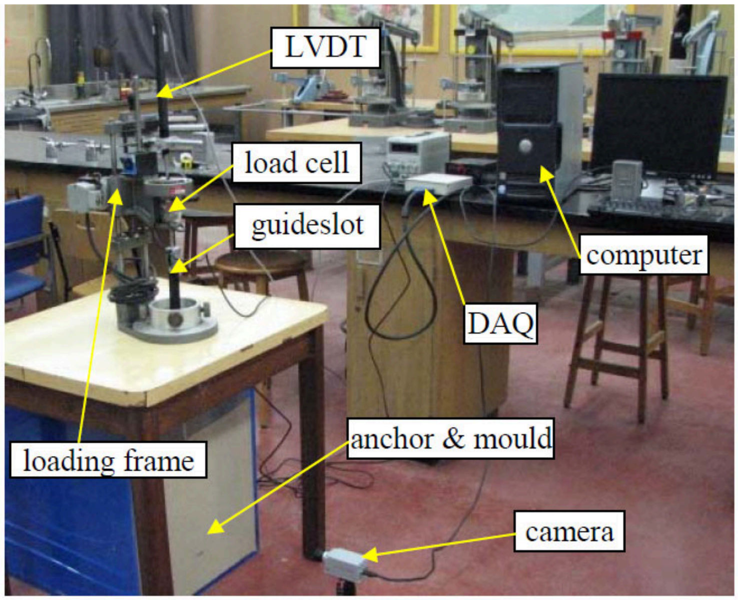

FIG.1. Test set-up for anchor uplifting and image capture

Table 1. Physical and geotechnical properties of sand used in the tests

State	Uniformity coefficient, C_u	Coef. of curvature C_c	Effective grain size D_{10} (mm)	Specific gravity, Gs	Relative density, Dr	Angle of friction (degree)
Loose	1.29	0.98	0.56	2.65	27	29^o
Dense	1.29	0.98	0.56	2.65	71	41^o

Sample Preparation

The density of soil samples is controlled by pouring and tamping. As for the loose sample, first, a 50 mm thick sand bed is first placed at the bottom of the mould. Second, the semicircular anchor is set on the sand bed and aligned vertically through the guide slot and horizontally against the front window of the Plexiglas mould. Third, the top sand is prepared by the controlled pluviation method to pour sands from a 5 cm height through a funnel to the required embedment depth of anchor. As for the dense sample, the same steps are followed, but in the third step, the sand is compacted layer by layer by tamping until the final height is reached.

In order to investigate the influence from the embedment depth, the embedment ratio, H/D, varies from 1 to 9 in this research, where H is the anchor embedment depth, D is the anchor diameter. Only the results from an embedment ratio of 3 and 8 are reported in this paper.

Test Procedure

First, the data acquisition and image capture drivers are activated in the PC. Second, the camera is first set at a distance varying from 25 cm to 45 cm away with its optical axis perpendicular to the box front window and the image focus and the light intensity are set by adjusting the lens and the aperture. Since the image analysis is very sensitive to the changes in ambient light, the light source for illuminating the sand surface is the only one left on while the rest is off with a dark room during the tests. Third, the camera is set in an auto data acquisition mode with a desired image frame rate, 1 frame per second used in this study. The data acquisition for the load and the displacement are set at a 200 data per second rate. Fourth, the anchor is lifted up by rotating the handle while the images and data are acquired and imported to the computer for the future process. Fifth, the test is terminated until an apparent failure rupture or a significant reduction in uplift resistance is observed in the sample and no additional loading can be taken by the anchor.

DIGITAL IMAGE PROCESSING

Digital Image Correlation (DIC) is used in this study to calculate the displacement field between two consecutive images taken during anchor uplifting. DIC is a classic pattern recognition technique where two images are compared to obtain the relative displacement between them. DIC is widely used in many engineering fields to obtain spatial deformation patterns, albeit with several names, in particular Particle Image Velocimetry (PIV).

In this paper, the PIVview2c software is used to calculate the field displacement. This software has features to allow users to select the window size, cross-correlation algorithm, peak function, etc. More details can be found in PIVTEC (2006). Unless noted, the features used in this research are final window size 16 X 16 pixels, the multiple-correlation algorithm, and the multi-grid interrogation method.

RESULT ANALYSES

Loading Capacity of an Uplifting Anchor

The load vs. displacement curves for both loose and dense conditions are shown in Fig. 2. The uplift resistance shows a rapid increase with the displacement at the initial stage for anchors in both loose and dense conditions. The similar tendency is noticed regardless the embedment depth.

For anchors embedded in loose sand as shown in Fig.2, there are only two phases noted in the tests: the initial phase and the peak phase. The ultimate uplift resistance, although vibrating at a relative mild extent, stays at the peak value until the displacement reaches 10 mm. For dense samples, the third phase, softening, is noticed in addition to the two phases in the loose condition, where the uplift resistance, after arriving at the peak, showed a gradual decrease with the increasing displacement.

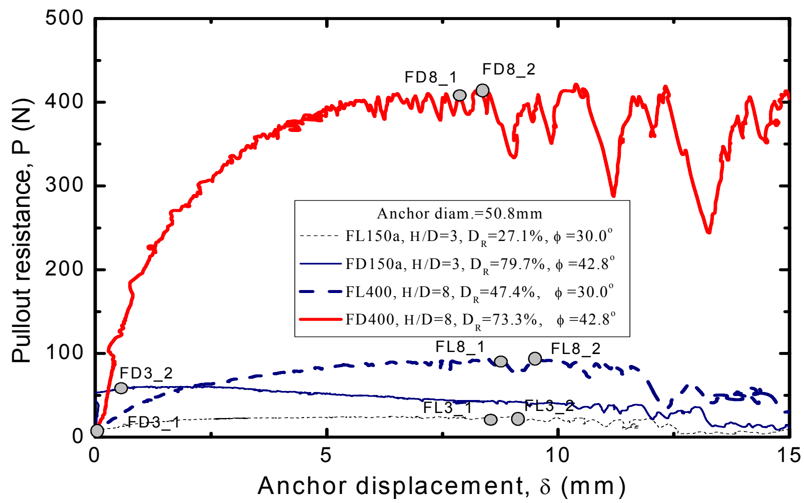

FIG. 2. The load vs. displacement curves for the anchor

Displacement Field around an Uplifting Anchor

The displacement fields at different phases can be calculated by cross-correlating two images taken at corresponding stages. In this paper, only the displacement fields at the peak phase for both embedment depths are presented. The labels in Fig. 2 note the pairs of images, for example FD3_2 represents the fine dense sand with an anchor embedment ratio of 3 and the image no. is 2. The displacement fields for both dense and loose conditions at the peak phase are shown in Fig. 3.

In loose sand, a similar displacement pattern is observed in both embedment depths, where the compaction is concentrated within a bell zone above the anchor. A compaction phenomenon is observed for the shallow anchor in loose sand. The displacement fields in both the embedment ratio of 3 and 8 are observed without significant change.

In dense sand, a significant change is observed in the displacement fields. For a shallow anchor with an embedment ratio of 3, a whole block above the anchor is mobilized to the soil surface with shearing blocks on both sides. For a deep anchor, a restrained displacement field is observed where the displacement does not penetrate to the soil surface.

Strain Field around an Uplifting Anchor

Strains can be deduced from predicted displacements. No apparent failure plane can be identified due to small displacement increments between two consecutive images. However, the failure plane can be assumed to occur along the locations experiencing maximum shear strains. The contours of shearing strain field for both loose and dense conditions are shown in Fig. 4.

In loose sand, a similar failure plane is observed in both embedment depths, which is similar to a punching shearing failure in shallow or deep foundations.

For a shallow anchor, a triangular wedge is formed from the maximum shear strains, while the failure planes extend outward in a deep anchor.

In dense sand, a significant change in the failure pattern is observed in a shallow anchor compared to a deep anchor. For a shallow anchor, two shear bands begin from the upper edge of the anchor plate and extend outward to the ground surface with an inclination angle with the vertical at approximately 20^{o}, which is around ½ ϕ. This failure mode is similar to ones proposed by other researchers. However, for a deep anchor in dense sand, the failure planes extends from the anchor edge and do not reach the soil surface.

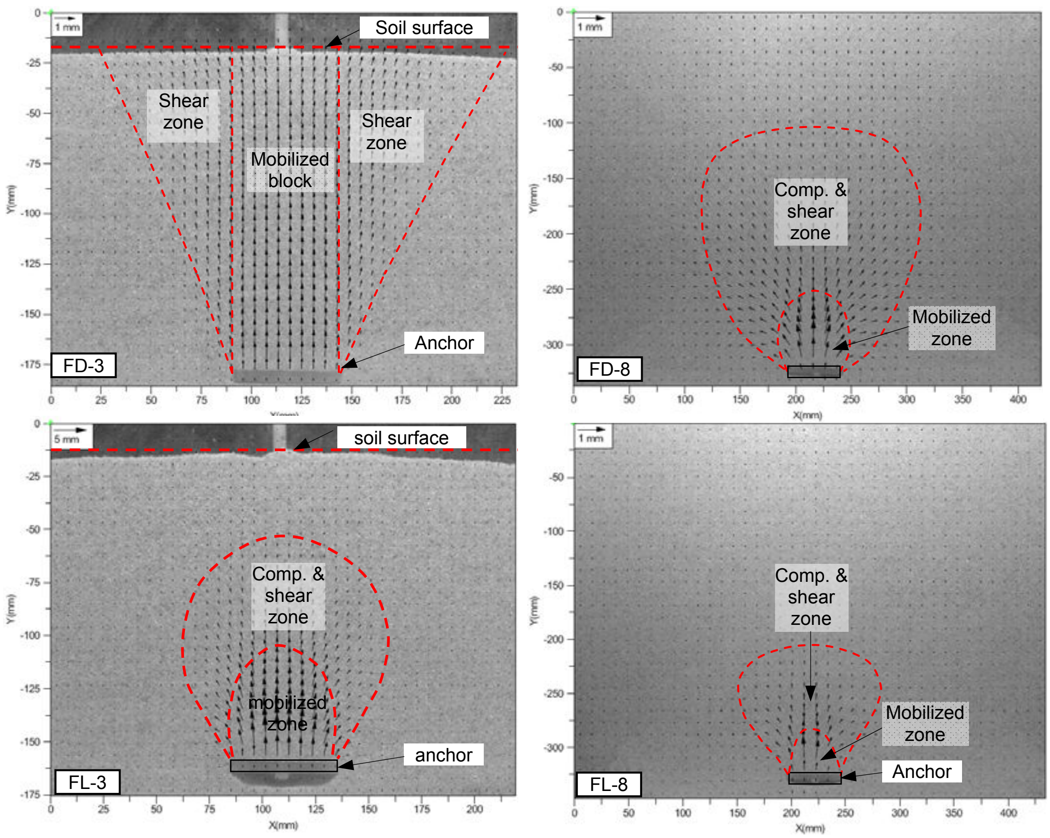

FIG. 3 The displacement fields at peak stage

CONCLUSIONS

This paper presents experimental investigation of the embedment depth on the failure model of an uplifting anchor. Soil displacement field around a scaled semi-circular anchor during uplifting is obtained using digital image correlation method. An optical test set-up is developed in this research to capture the deformation during loading, which consists of a camera, a loading frame, and a PC. Two dry sand samples are used in the investigation: one is in loose condition and the other in dense. A series of images are taken from the camera while the semi-circular anchor is being uplifted against the side-window of a Plexiglas mould. The displacement fields are calculated using DIC and the corresponding strain fields are deduced from the displacement fields.

There are distinctive differences between the displacement fields between the loose and dense conditions. In the loose samples a similar punching shear failure mode is observed regardless of the anchor depth. In dense sand, a restrained failure mode is observed in a deep anchor compared to the failure plane extending to ground surface in a shallow anchor.

This study improves the understanding of the failure and loading capacity of an uplift anchor in cohesionless soil.

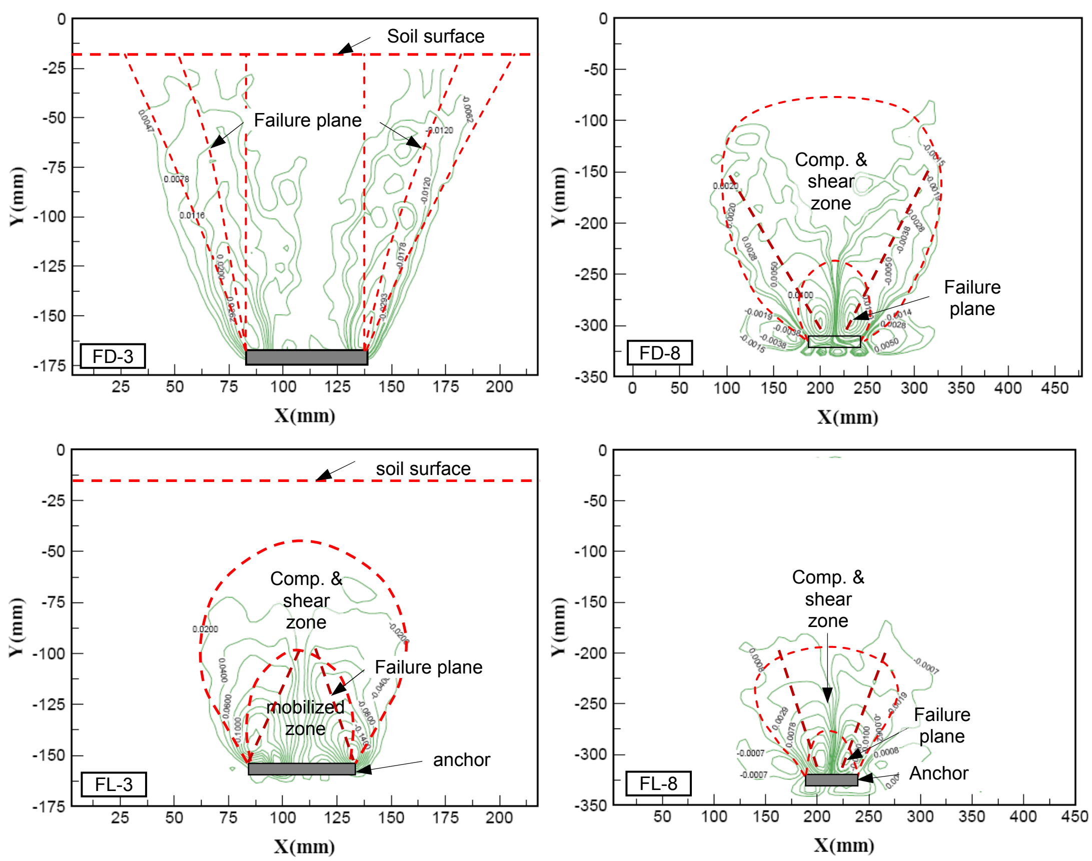

FIG.4. The shear strain contour field

ACKNOWLEDGEMENTS

The authors acknowledge the financial support of the Seed Fund awarded to the first author. The authors also want to thank the China Scholarship Council for the scholarship awarded to the second author during his one-year study at Ryerson University.

REFERENCES

Balla, A. (1961). "The resistance to breaking out of mushroom foundations for pylons." *Proc. of the 5th ICSMFE*, Paris, 569-576.

Carr, R.W. and Hanna, T. H. (1971). "Sand movement measurements near anchor plates." *J. of the Soil Mech. and Found. Div., ASCE*, 97, 833-840.

Hanna, T. H., Sparks, R., and Yilmaz, M. (1972). "Anchor behavior in sand." *American Society of Civil Engineers, Journal of the Soil Mechanics and Foundations Division*, 98(SM11), 1187-120.

Ilamparuthi, K., Dickin, E. A., and Muthukrisnaiah, K. (2002). "Experimental investigation of the uplift behaviour of circular plate anchors embedded in sand." *CGJ*, 39(3), 648-664.

Meyerhof, G. G., and Adams, J. I. (1968). "The ultimate uplift capacity of foundations." *CGJ*, 5, 225-244.

Murray, E. J., and Geddes, J. D. (1987). "Uplift of anchor plates in sand." *J. of Geotech. Eng., ASCE*, 113(3), 202-215.

PIVTEC GMBH (2006). *PIVview User Manual,* Ver.2.4, http://www.pivtec.com/.

Saeedy, H. S. (1987). "Stability of circular vertical anchors." *CGJ*, 24(3), 452-456.

Sutherland, H. B. (1965). "Model studies of shaft raising through cohesionless soils." *Proc.of the 6th ICSMFE,* Montreal, 410-413.

Sutherland, H. B. (1988). "Uplift resistance of soils." *Geotechnique*, 38(4), 493-516.

Vesic, A. S. (1971). "Breakout resistance of objects embedded in ocean bottom." *ASCE, J. of the Soil Mech. and Found. Div.*, 97(9), 1183-1203.

Elucidating the Uplift Behavior of Underreamed Anchor Groups in Sand

Shih-Tsung Hsu

Associate Professor, Department of Construction Engineering, Chaoyang University of Technology, 168, Jifong E. Rd., Wufong Township, Taichung County, 41349, Taiwan. E-mail: sthsu@cyut.edu.tw.

ABSTRACT: Both numerical analyses and model tests were performed to study the interactive behavior of underreamed anchor groups in sand. A constitutive model named *SHASOVOD* which could simulate the strain hardening-softening and the volume dilatancy of cohesionless soils during shearing, in conjunction with $FLAC^{3D}$ software to execute the numerical analysis. The results measured from model anchor tests were compared with those calculated by numerical analyses.

The load-displacement behaviors calculated numerically consisted with those measured by the tests of the single anchor and the paired anchors. According to the numerical results, the interference induced by the paired anchors is smaller than that induced by the triple anchors. When the spacing between neighboring anchors is small (such as S_h=2D, D is the anchor diameter), yielding zones of soil around each anchor highly superpose, the average capacity of an anchor group is much smaller than the capacity of a single anchor. The superposition of yielding zones decrease with horizontal spacings; the behavior of each anchor in the anchor group tends to a single anchor as the horizontal spacings exceed a threshold value of 10D.

INTRODUCTION

To solve the problem of overturning, the construction of viaducts or bridges commonly utilizes those pile groups or anchor systems. Deep excavations are usually supported by those diaphragm walls with internal braces or tieback anchors. A system of tieback anchors is more economic and provides a larger working space. Vertical anchors are employed to tie down basements against ground-water uplift pressure or to counterbalance eccentric loads that act on foundation mats. Anchors are seldom to be applied in single, and are commonly utilized in a group. Although anchors are applied extensively, the interactive behavior of anchor groups is rarely to be investigated.

As shown in Fig. 1a, a mechanically underreamed anchor meets both the requirements of short length and high anchorage capacity (Liao, 1993). The fixed length is form by the underreamed blade. The device with 4 blades keeps close initially. As the drilled rod drill to predetermined length, all blades open and rotate simultaneously to enlarge the fixed length. After the enlarging, the drilled is replaced by the strand assembly which is connected with the swivel, after that, a grout with water/cement ratio *W/C* of 0.5 is pressurized at 1MPa to form the fixed length. The applied load is passed through the sheathed strands to the bladed device which is used as an anchorage body; therefore, the grouting body undergoes compressive stress, and can be classified as a type of a compression anchor.

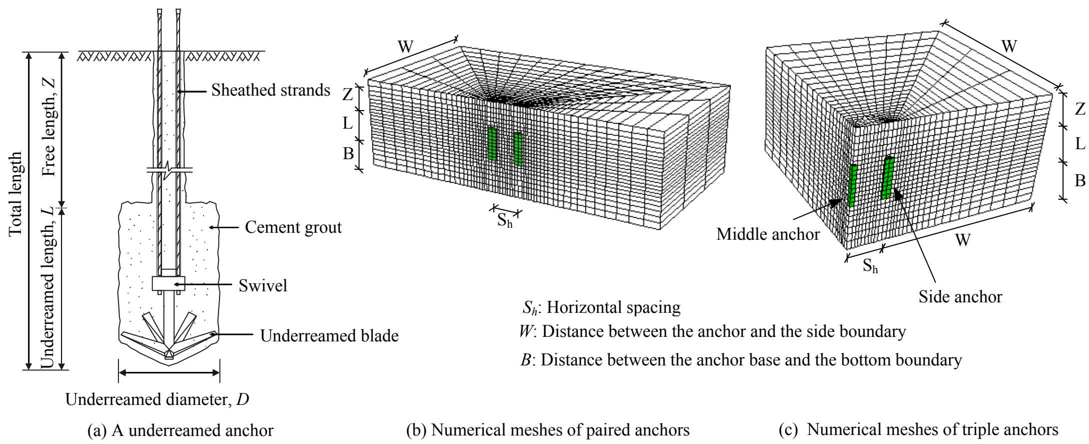

Fig. 1. Construction of the underreamed anchor and typical meshes for analyzing paired and triple anchors

CONSTITUTIVE MODEL AND NUMERICAL PROCEDURE

The sand specimen which was sampled from Yi-Lan had a D_{10} of 0.16 mm, D_{30} of 0.25 mm, D_{60} of 0.39 mm, a coefficient of uniformity of 2.44, a coefficient of gradation of 1.0 and a fines content (< #200) of 1%. It was an *SP* soil; its specific gravity G_s was 2.69; its maximum dry density was 17.34 kN/m^3, and its minimum dry density was 13.70 kN/m^3.

The constitutive model that was proposed by Hsu and Liao (1998) was adopted herein to model the stress-strain behavior of sand. The yield function *f* is

$$f = \sigma_1 - \sigma_3 \frac{1+\sin\phi^*}{1-\sin\phi^*} \quad (1)$$